

Small RNA deep sequencing identifies viral microRNAs during malignant catarrhal fever induced by alcelaphine herpesvirus 1

Océane Sorel,¹ Lee Tuddenham,² Françoise Myser,¹ Leonor Palmeira,^{1†} Pierre Kerkhofs,³ Sébastien Pfeffer,² Alain Vanderplasschen¹ and Benjamin G. Dewals¹

Correspondence
Benjamin G. Dewals
bgdewals@ulg.ac.be

¹Fundamental and Applied Research in Animals and Health (FARAH), Immunology–Vaccinology, Faculty of Veterinary Medicine (B43b), University of Liège, Belgium

²Architecture et Réactivité de l'ARN – UPR 9002, Institut de Biologie Moléculaire et Cellulaire du CNRS, Université de Strasbourg, 15 rue René Descartes, F-67084 Strasbourg Cedex, France

³Veterinary and Agrochemical Research Center (CODA-CERVA), Brussels, Belgium

Alcelaphine herpesvirus 1 (AIHV-1) is a γ -herpesvirus (γ -HV) carried asymptotically by wildebeest. Upon cross-species transmission, AIHV-1 induces a fatal lymphoproliferative disease named malignant catarrhal fever (MCF) in many ruminants, including cattle, and the rabbit model. Latency has been shown to be essential for MCF induction. However, the mechanisms causing the activation and proliferation of infected CD8⁺T cells are unknown. Many γ -HVs express microRNAs (miRNAs). These small non-coding RNAs can regulate expression of host or viral target genes involved in various pathways and are thought to facilitate viral infection and/or mediate activation and proliferation of infected lymphocytes. The AIHV-1 genome has been predicted to encode a large number of miRNAs. However, their precise contribution in viral infection and pathogenesis *in vivo* remains unknown. Here, using cloning and sequencing of small RNAs we identified 36 potential miRNAs expressed in a lymphoblastoid cell line propagated from a calf infected with AIHV-1 and developing MCF. Among the sequenced candidate miRNAs, 32 were expressed on the reverse strand of the genome in two main clusters. The expression of these 32 viral miRNAs was further validated using Northern blot and quantitative reverse transcription PCR in lymphoid organs of MCF-developing calves or rabbits. To determine the concerted contribution in MCF of 28 viral miRNAs clustered in the non-protein-coding region of the AIHV-1 genome, a recombinant virus was produced. The absence of these 28 miRNAs did not affect viral growth *in vitro* or MCF induction in rabbits, indicating that the AIHV-1 miRNAs clustered in this non-protein-coding genomic region are dispensable for MCF induction.

Received 23 July 2015
Accepted 27 August 2015

INTRODUCTION

Malignant catarrhal fever (MCF) is an acute, sporadic and fatal pan-systemic lymphoproliferative disease of a variety of species of the order Artiodactyla, including cattle. The main causative agents of MCF are two γ -herpesviruses (γ -HVs) that are grouped in the genus *Macavirus*

[†]Present address: Department of Endocrinology, University of Liège, B-4000 Liège, Belgium.

The data discussed in this paper have been deposited in NCBI's Gene Expression Omnibus (GEO) and are accessible through GEO Series accession number GSE71056.

Four supplementary figures and two supplementary tables are available with the online Supplementary Material.

(*malignant catarrhal*), ovine herpesvirus 2 (OvHV-2) and alcelaphine herpesvirus 1 (AIHV-1). These viruses cause no apparent disease in their natural host species. Sheep are naturally infected by OvHV-2, which is responsible for the sporadic sheep-associated form of MCF. Wildebeest are persistently infected with AIHV-1, the causative agent of the wildebeest-derived form of the disease (Plowright, 1990; Plowright *et al.*, 1960). The prevalence of AIHV-1 infection in wildebeest is close to 100 % and transmission to MCF-susceptible species is mainly believed to occur during the calving period and in the first months of life (Plowright, 1965a, b). Recent data demonstrated that MCF is caused by the activation and proliferation of latently infected CD8⁺T cells, resembling a peripheral T cell lymphoma (Dewals & Vanderplasschen, 2011; Dewals

et al., 2008, 2011; Palmeira *et al.*, 2013). Infected lymphocytes collected from animals developing MCF can be propagated *in vitro* in the presence of interleukin 2 (IL-2) and display a 'large granular lymphocyte' phenotype (Swa *et al.*, 2001). These lymphoblastoid cell lines (LCLs) can be used to amplify the number of infected cells *in vitro*. Although expression of latency-associated ORF73 expression has been shown to be essential for MCF induction (Palmeira *et al.*, 2013), the actual mechanisms involved in the activation and proliferation of infected CD8⁺T cells are yet to be identified. MCF can be experimentally induced in rabbits, where the observed lesions are indistinguishable from those described in MCF-susceptible species (Buxton & Reid, 1980).

In general, γ -HV latency is not associated with disease development. However, in particular circumstances depending on the viral species and the infected host, latency in lymphocytes can result in malignant lymphocyte activation and proliferation (Barton *et al.*, 2011; Ensser & Fleckenstein, 2005; Russell *et al.*, 2009). Latency is finely regulated by a highly restricted viral gene expression programme within the infected cells, which enables γ -HVs to evade continuous active immune surveillance and persist in the host. Although the host immune system generally controls infection, severe latency-associated lymphoma or lymphoma-like diseases can occur. One component of regulation of latent infection is the transcription of non-coding RNAs (ncRNAs), such as microRNAs (miRNAs) (Pfeffer *et al.*, 2004, 2005). miRNAs are a large family of small ncRNAs (~22–25 nt) that regulate gene expression typically through imperfect binding to the 3'-untranslated region of target mRNAs, resulting in mRNA degradation, sequestration and translational repression (Bartel, 2009).

An increasing number of studies have demonstrated the widespread role of non-coding RNAs, including miRNAs, in cancer induction (Croce, 2009; Ventura & Jacks, 2009). The identification of miRNAs encoded by many oncogenic viruses, including herpesviruses, polyomaviruses and some retroviruses, suggested that they could contribute to the pathogenesis of virus-induced cancers (Grey, 2015; Kincaid & Sullivan, 2012; Rosewick *et al.*, 2013; Zhu *et al.*, 2013). Some herpesvirus-encoded miRNAs have been shown to regulate both cellular and viral processes, including cell cycle and lymphomagenesis (Dölken *et al.*, 2010; Seto *et al.*, 2010; Stik *et al.*, 2010; Suffert *et al.*, 2011; Zhao *et al.*, 2011). Interestingly, a small cluster of EBV-encoded miRNAs has been shown to promote its transforming properties (Feederle *et al.*, 2011). Although very little is known on the actual functions of γ -HV-encoded miRNAs *in vivo*, two recent studies suggested that murid herpesvirus 4 (MuHV-4)-encoded miRNAs are not essential for viral replication or latency establishment in immunocompetent mice but potentiate the acute pathology induced by MuHV-4 infection in IFN- γ -deficient mice (Diebel *et al.*, 2015; Feldman *et al.*, 2014).

Prediction analysis of pre-miRNAs in different γ -HV genomes identified as many as 70 and 88 potential hairpins encoded by AIHV-1 and OvHV-2, respectively (Walz *et al.*, 2010). These predicted pre-miRNAs are globally clustered downstream of the DNA polymerase gene in a large non-protein-coding region of the genome in both virus species. However, the sequences were highly divergent between the two virus species. Sequencing data of OvHV-2-infected LCL identified the expression of 45 potential viral miRNAs. Among them, the expression of 35 miRNAs could be validated using reverse transcription PCR (RT-PCR) and Northern blotting. Notably, 30 of the expressed OvHV-2 miRNAs clustered together on the reverse strand of the genome in a large non-protein-coding region between ORF11 and ORF17 (Nightingale *et al.*, 2014; Riaz *et al.*, 2014). To date, whether OvHV-2 miRNAs are involved in sheep-associated MCF is not known.

Here, we first cloned small RNAs from total RNA isolated from a lymphoblastoid cell line propagated from a calf developing MCF after AIHV-1 infection, which was followed by high-throughput sequencing. A total of 36 AIHV-1 small RNAs were identified, among which 32 were miRNA candidates, all encoded by the reverse strand of the viral genome and organized in two main clusters. Expression of viral miRNAs could be detected using Northern blot analysis and quantitative PCR (qRT-PCR) in lymphoid organs of MCF-developing calves or rabbits. To determine the concerted genetic contribution of 28 viral miRNAs clustered in the non-protein-coding region of the AIHV-1 genome in the pathogenesis of MCF, a recombinant virus deleted of the entire cluster was generated. The absence of these 28 miRNAs did not affect viral growth *in vitro* or MCF induction in rabbits, demonstrating that AIHV-1 miRNAs clustered in the non-protein-coding genomic region between ORF11 and ORF17 are not directly involved in MCF pathogenesis.

RESULTS AND DISCUSSION

Induction of MCF in calves and propagation of AIHV-1-infected lymphoblastoid cell lines

Samples from an experiment previously described were used (Palmeira *et al.*, 2013). Calves were experimentally infected with AIHV-1 WT C500 strain to induce MCF. All AIHV-1-infected calves developed typical prostration, nasal discharge, lymphadenopathy and severe persistent hyperthermia at 12.2 ± 0.5 days post-infection (p.i.) (Fig. 1a). AIHV-1 infected animals also developed typical MCF with lymph node (LN) hypertrophy (Fig. 1b), increased CD8⁺T cell percentages in peripheral blood and LN (Fig. 1c), increased IFN- γ production and characteristic infiltrations of lymphoblastoid cells in the perivascular spaces of many tissues (Palmeira *et al.*, 2013). LCLs (also termed 'large granular lymphocytes') were established by culturing peripheral mononuclear cells in the presence of recombinant human IL-2 (hIL-2) (Swa *et al.*, 2001).

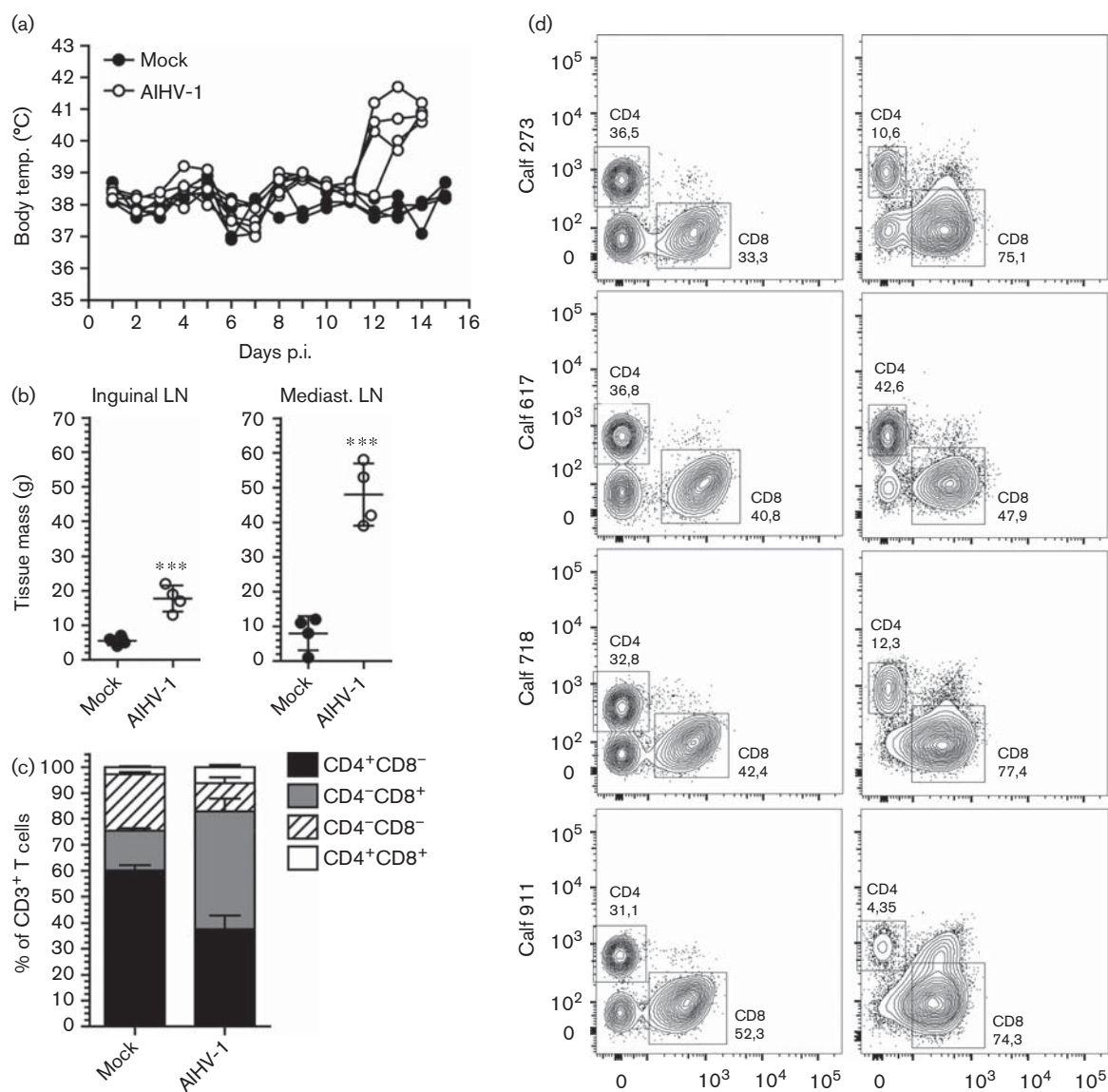


Fig. 1. Induction of MCF in calves. (a) Body temperature recorded daily after intravenous inoculation of two groups of four calves with mock-infected BT cells (mock, solid symbols) or cells infected with the AIHV-1 WT C500 strain (AIHV-1, open symbols). Calves were euthanized at 14 (AIHV-1) and 16 (mock) days p.i. (b) Inguinal and mediastinal LN mass at time of death. (c) Percentages of CD4⁺ and CD8⁺ cells in the gated CD3⁺ T cell population in inguinal LN at time of euthanasia. (d) Multicolour flow cytometry analysis of CD4⁺ and CD8⁺ T cells in PBMC before and after propagation in culture with rhIL-2 (10 ng ml⁻¹). Gate was placed on CD3⁺ T cells. LCLs propagated from all calves showed >90 % CD3⁺ T cells. Error bars in (b) and (c) indicate SE.

The obtained LCLs were propagated in the presence of hIL-2 and showed significant enrichment of CD8⁺ T cells (Fig. 1d). This procedure enables the enrichment of infected lymphocytes as well as a significant increase of the total number of cells.

Identification of AIHV-1-derived small RNAs

To identify viral miRNAs encoded by AIHV-1, we performed small RNA cloning and deep sequencing of one

selected LCL propagated from calf 718, namely LCL718. Although viral infection was already detected to be high in the peripheral blood of calves developing MCF (Palmeira *et al.*, 2013), we further confirmed that LCL718 cells were infected and expressed high levels of the latency-associated ORF73 RNA (not shown). Total RNA from LCL718 cells was size fractionated in a polyacrylamide gel, and RNA species 19 to 24 nt in size were cloned and sequenced as previously described (Tuddenham *et al.*,

2012). In total, 35 404 509 reads were obtained. Following collapsing of the reads into sequence tags, 94.2 % of the resulting 2 425 556 unique sequence tags could be mapped to either the bovine or the AIHV-1 genome, and were categorized into RNA classes based on sequence annotation (Table 1). Allowing two mismatches for the alignment to the viral genome, 1.5 % of the total reads (corresponding to 36 383 sequence tags) mapped to the AIHV-1 genome. About 28.8 % of the sequenced reads corresponded to cellular miRNAs, suggesting that among all miRNAs expressed in LCL718 cells, around 5.2 % were of viral origin.

Distribution of AIHV-1 small RNA sequences across the genome

Sequences were mapped to the AIHV-1 C500 reference genome (GenBank accession no. NC_002531.1). The AIHV-1 genome consists of a unique long region (LUR) of 130 608 kbp flanked by poly-repetitive regions of 1118 bp (prDNA) (Ensser *et al.*, 1997). The distribution of AIHV-1 small RNA sequences across the genome revealed that the viral sequences mostly derived from the reverse strand of the genomic DNA and clustered into two main regions, as previously predicted (Walz *et al.*, 2010). The first region consisted of four miRNA candidates at the far-left end of the

genome and included small RNAs complementary to the A1 gene coding sequence (Fig. 2a, b). The second region included 28 potential miRNAs clustering into a region devoid of any predicted ORF, between ORF11 and ORF17 (Ensser *et al.*, 1997; Walz *et al.*, 2010) (Fig. 2a, b). Two additional isolated small RNA sequences mapped to the forward strand of the genome, in the same region and into the ORF20 coding sequence, respectively (Fig. 2a). Sequencing data suggested that these two small RNAs were less abundant. Finally, two small RNA sequences also mapped to the prDNA region (Table 2). These data suggested that up to 36 miRNA candidates are expressed in AIHV-1-infected LCLs, among which 31 were previously predicted (Walz *et al.*, 2010). Here we further focused on the identification of AIHV-1 miRNAs of the two major clusters of small RNAs expressed from the reverse strand of the viral genome.

Identification of AIHV-1 miRNAs

Previous prediction analysis identified putative pre-miRNA sequences in the AIHV-1 genome (Walz *et al.*, 2007). Among the 36 small RNAs that were expressed in LCL718 cells, 31 matched with predicted pre-miRNA sequences (Table 2). The sequences that were cloned multiple times and had characteristic 5' homogeneity were assessed manually for their ability to fold into typical stem-loop precursor structures using Mfold (Zuker, 2003) (Fig. S1, available in the online Supplementary Material). Thirty-two sequences mostly deriving from predicted classical pre-miRNA stem-loop structures and that matched perfectly to the AIHV-1 genome were selected for validation. These miRNA candidates were numbered according to their position in the reverse strand of the genome (Table 2). For most candidates, both 5p and 3p forms of the miRNA were sequenced. For each pre-miRNA, the predicted mature miRNA having the highest number of reads was selected for further analyses. To validate these candidates, we performed Northern blot analysis of total RNA extracted from LCL718 and from peripheral LN of calves developing MCF. We first selected miRNA candidates AIHV-miR-1, 3–11, 15, 20–23 and 27–32, for which a significant high number of reads could be detected in LCL718 cells (Fig. 2, Table 2). Northern blot analysis confirmed the expression of these selected miRNAs in LCL718 cells and also demonstrated that they could be detected in LN of MCF-developing calves (Fig. S2). Total RNA from peripheral LN of a mock-infected calf was used as a control. Finally, we used a qRT-PCR approach to determine the relative expression of AIHV-miRNAs in RNA extracted from LCL718 (Fig. 3a). The relative expression levels of the viral miRNAs obtained by RT-PCR (Fig. 3a) globally supported the sequencing data (Fig. 2, Table 2), suggesting the robustness and specificity of this quantitative approach. However, some variation could be observed, such as AIHV-miR-20, 22, 26, 31 and 32, for which the RT-PCR results did not fully support the sequencing data. These discrepancies could be explained by variable efficiency in the sequencing procedure and/or specificity of the primer pairs. To further

Table 1. Distribution of the mapped reads against the cellular and viral databases

MtRNA, mitochondrial RNA; Mt_tRNA, mitochondrial tRNA; scRNA, small cytoplasmic RNA; snRNA, small nuclear RNA; snoRNA, small nucleolar RNA; teloRNA, telomerase RNA.

Organism	Target	Percentage of reads
<i>Bos taurus</i>	miRNA	28.8
	Genome	22.5
	rRNA	19.1
	tRNA	6.9
	mRNA	5.3
	ncRNA	2.6
	snoRNA	1.7
	MtRNA	0.9
	snRNA	0.8
	Mt_tRNA	0.2
	Repeats	<0.1
	Ψ gene	<0.1
	Retrotransposed	<0.001
	teloRNA	<0.000 1
AIHV-1	scRNA	<0.000 01
	LUR	1.5
	prDNA	<0.001
Ambiguously mapped reads		3.8
Unmapped reads		5.8

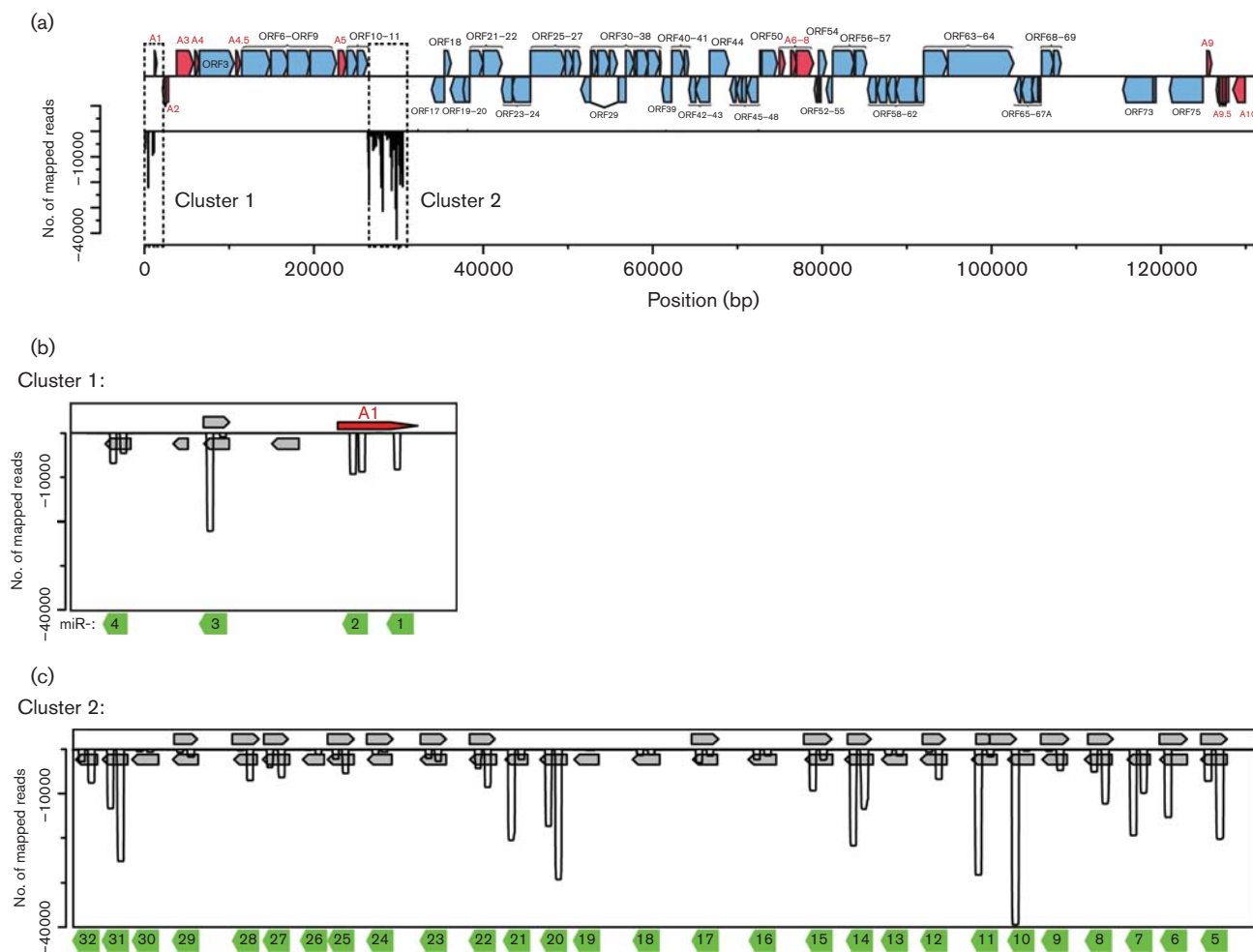


Fig. 2. Genomic distribution of AIHV-1 small RNA sequences. (a) Small RNA cloning from total RNA of LCL propagated from a calf infected by the AIHV-1 C500 WT strain and developing MCF (LCL718). Predicted ORF are represented by the blue boxes and AIHV-1 specific ORFs are depicted in red. Small RNA reads are mapped on the genome relative to their position and abundance. (b) Inset zooms of identified small RNA cluster 1 and 2. Small RNA reads are mapped on the reverse strand of the genome relative to their position (from 5'- to 3'-end) and abundance. The grey boxes represent previously predicted pre-miRNA (Walz *et al.*, 2010). Negative values represent reads mapping on the reverse strand of the genome.

investigate the expression of viral miRNAs during MCF, we extracted RNA from the LN of calves developing MCF to perform RT-PCR analyses (Fig. 3b). The results showed that most AIHV-miRNAs candidates are expressed in the peripheral LN of calves developing MCF and correlate with the expression levels observed in LCL718 cells. Total RNA from peripheral LN of uninfected calves was used as a control and melting curve analysis was performed in order to further verify the specificity of the PCR amplification (Fig. S3). Rabbits are used as an experimental model for MCF induction (Palmeira *et al.*, 2013). We therefore verified whether the candidate viral miRNAs were also expressed in the lymphoid tissue of a rabbit infected with the AIHV-1 WT BAC-excised strain (Dewals *et al.*, 2006). We observed a similar expression pattern of the sequenced miRNAs in rabbit LN and spleen (Fig. 3c, d). Together,

these results demonstrated that the AIHV-1 genome encodes miRNAs that are expressed in lymphoid tissues during MCF in calves and rabbits.

AIHV-1 miR-31-5p is a potential orthologue of miR-291b-3p

Herpesviruses such as Marek disease virus (MDV) or Kaposi's sarcoma-associated herpesvirus (KSHV) express miRNAs that share full homology in their seed sequences (nt 2–7) with some cellular miRNAs. For instance, MDV-miR-M4 (Zhao *et al.*, 2009) or KSHV-miR-K12-11 (Gottwein *et al.*, 2007) have been shown to be functional orthologues of the cellular miR-155, an miRNA involved in lymphocyte activation. Here, we used miRBase (<http://www.mirbase.org>) to search for homologies in seed regions

Table 2. AIHV-1 small RNA sequences, genomic locations, and distribution in the library

The predominantly cloned sequences are indicated. 5p, 5' arm of the hairpin precursor; 3p, 3' arm of the hairpin precursor. Positions are given relative to the published genomic sequence of the C500 strain of AIHV-1. Small RNAs of ≤ 16 bp were not considered as miRNA and are displayed as 'miR'.

AIHV-1 miRNA	Cloned sequence (major form)	Strand	Size (nt)	No. of reads	Genomic location	Walz <i>et al.</i> (2010)*
Cluster 1						
miR-4-5p	UCUGCUGCGCGGCGCUUCUUU(CU)	—	21	1878	122–142	Pre-miR-1
miR-4-3p	GAGGAGCCUCGCGACGGCAGAGA(A)		22	5273	84–105	
miR-3-5p	CAGAGACCGCACGGGUGUUUCU	—	22	407	486–507	Pre-miR-3
miR-3-3p	UCACACCCAGGCGGUCUCUGCA(A)		22	7779	433–460	
miR-2-5p	UUAAGAAAUAUAGGCUCAAGGU(U)	—	22	3994	996–1017	/
miR-2-3p	UCUUGUGCCUAGAUAUUCUUAUA		22	4929	963–984	
miR-1-5p	UACAAGGGCUAAGCAUGAGCU(GU)	—	21	4086	1126–1146	/
Cluster 2						
miR-32-5p	UGCGGGGUUGUGGGAAGCAGACG	—	23	5470	26392–26414	Pre-miR-7
miR-32-3p	UCUGCUUCGCCAUCUCCGUAC		21	375	26358–26378	
miR-31-5p	AAAGUGCACCCUGGUUGUUUG(UG)	—	22	11043	26500–26522	Pre-miR-8
miR-31-3p	UAAAACCUCGGGUGCACUUAU		21	7139	26464–26484	
miR-30-5p	UGUUGGCACCUGGGUUAUUAUUAU	—	23	196	26610–26632	Pre-miR-9
miR-30-3p	UGUAAUAGCACUGUGUGCUAC		21	26	26572–26592	
miR-29-5p	UGGAAAAGCUAUGUUUCAAUAACG	—	24	1033	26760–26783	Pre-miR-10
miR-29-3p	UAUUUGAAAAUAGCUUUUCCG		21	206	26722–26742	
miR-28-5p	GUUAUGCAUGAGCAUAACUGUU	—	22	6528	26980–27001	Pre-miR-11
miR-28-3p	ACAGUUUUGACCAUGCUAGCC		21	24	26946–26966	
miR-27-5p	UAGGCUAGUCUGGACAAAACACU	—	23	4784	27096–27111	Pre-miR-12
miR-27-3p	UGUUUUGUACAGGCUACCUAGC		22	1592	27054–27075	
miR-26-5p	UAGCUUGUGUGUUGUGUCUGU	—	21	892	27234–27254	Pre-miR-13
miR-25-5p	UAAGAGCUUUGGCGAAGGCU(CU)	—	21	2403	27334–27354	Pre-miR-14
miR-25-3p	AUCUUUGCCAAGUACUCUGGU	—	21	1196	27298–27318	
miR-24-5p	CACGAUAGUUUAGAAAAAUCUGU	—	24	216	27476–27499	Pre-miR-15
miR-24-3p	UGAUUUUUACUAUGCUAUCAGA		22	801	27445–27466	
miR-23-5p	AGAUAGUUUGGGGGAGGCCUUU	—	22	654	27676–27697	Pre-miR-16
miR-23-3p	UGGCUCAGCCAAACUAUCACG		21	941	27642–27662	
miR-22-5p	UGAUUCCUAAUGGAGGACU(UU)	—	21	3724	27861–27881	Pre-miR-17
miR-22-3p	AGGUGCUACAUAAGAUAUGA		22	1445	27826–27847	
miR-21-5p	UGUCAGUUACAGCAGGAAUUGUU	—	23	1792	27984–28006	Pre-miR-18
miR-21-3p	CAUCCGGGCUUUAACUGACAAGC		24	14227	27947–27970	
miR-20-5p	GAUAGAUUGGGUUAGGAUCUGU	—	22	24011	28122–28143	Pre-miR-19
miR-20-3p	AGAUCUUGUCUCAAUCUGUCUU		22	2320	28086–28107	
miR-19-5p	UGAUAGCUUAAGGUGCUCUCUG	—	22	60	28245–28266	Pre-miR-20
miR-18-5p	CAGUAGUUGGAAGUACCCUAUU	—	22	666	28465–28486	Pre-miR-21
miR-18-3p	AAUAAGGUGCAGCCGACUCUUA		22	253	28425–28446	
miR-17-5p	UAGUGGUCAGGCGAGUCUUAUU	—	22	964	28672–28693	Pre-miR-22
miR-17-3p	UACGACGCGUCUGACUACUCC		21	826	28634–28654	
miR-16-5p	UAAUGGUUGCCUGUGCUAUAUU(U)	—	22	750	28875–28897	Pre-miR-23
miR-16-3p	AUUGGCGCAGUUAACUAUUGC		21	411	28838–28858	
miR-15-5p	GAGCACCAUCAGUAGUUAUGUGU	—	23	972	29072–29094	Pre-miR-24
miR-15-3p	AAUAACUGCUGACAGUGCAAGU		22	7609	29035–29056	
miR-14-5p	AUCCAGUACACAAGCUUCCCCCGU	—	24	2814	29218–29241	Pre-miR-25
miR-14-3p	CGGGUGCGAGUGUACUGGCAU		21	6575	29178–29198	
miR-13-5p	CAAGUACACUACGUACACGCGGU	—	24	493	29341–29364	Pre-miR-26
miR-13-3p	UGCAGUGUUGCUUAGUGUCUUAG		24	235	29302–29325	
miR-12-5p	UAGUUACAUUGACUGGUAAUA	—	21	4535	29481–29501	Pre-miR-27
miR-12-3p	GUUACCAGUUUUUGUACCAG		20	14	29448–29467	
miR-11-5p	GCGGUACUGGGGUUGUAAAAGA	—	22	1022	29663–29684	Pre-miR-28
miR-11-3p	GUUAACAUCCCCAUAUCGGU(U)		21	14878	29481–29501	
miR-10-5p	ACGGUGCAGUAACUGAUUAAGA	—	22	139	29790–29811	Pre-miR-30

Table 2. cont.

AlHV-1 miRNA	Cloned sequence (major form)	Strand	Size (nt)	No. of reads	Genomic location	Walz <i>et al.</i> (2010)*
miR-10-3p	UAUAACGGAACACCUGCAUCGGCU		24	17758	29751–29773	
miR-9-5p	UGAAGCAGGCUAUCUCUCACCUG	–	23	708	29909–29930	Pre-miR-31
miR-9-3p	CAAGUGCAAGUGGCCUGCCUCAA		22	45	29870–29892	
miR-8-5p	AAUCAGACGGCUUGUGCAUAAGCU	–	24	3183	30068–30091	Pre-miR-32
miR-8-3p	UUAUGCACGGCUACCUGGUAG		21	2876	30030–30050	
miR-7-5p	AGACAGACAGUGAGCGGGUGCG	–	22	2295	30205–30226	Pre-miR-33
miR-7-3p	CAAUCCACUCCUGUCUGUCACU		23	5923	30167–30189	
miR-6-3p	UAAUCUGCAAACUUCUGUCCCCU	–	23	10632	30291–30312	Pre-miR-34
miR-5-5p	AAUCGAGAAAGGCACUCCUACCGG	–	25	8866	30472–30496	Pre-miR-35
miR-5-3p	UGUGGGUCUAGUGUCCUUCGAGA		24	5657	30431–30454	
Isolated						
miR-33-5p	UGAGCAACACUCCUGCCCCAG	+	22	64	32375–32395	Pre-miR-36
'miR'-34-5p	AUCCCGGGGCCGAGGG	+	16	210	38132–38147	
pr-DNA						
'miR'-35-5p	CCCCGCCCCCGCUCU	+	16	48	82–97	
miR-36-5p	UCCCCCGCGGGGGCCCCGGG	+	20	1926	252–271	

*Correspondence with predicted pre-miRNAs in Walz *et al.* (2010).

of the expressed AlHV-1 miRNAs. We found that the AlHV-1 miR-31-5p seed region fully matched the seed region of the cellular miR-291b-3p (Fig. 4). This specific miRNA is part of the miR-290–295 cluster, a cluster that is essentially expressed during embryonic development (Lüningschrör *et al.*, 2012) and has been shown to mediate resistance to autophagic cell death of melanoma cells (Chen *et al.*, 2012). It remains to be determined whether AlHV-1 miR-31-5p is a functional orthologue of miR-291b-3p and its role in AlHV-1 infection.

Deletion of cluster 2 miRNAs does not affect AlHV-1 replication *in vitro* nor MCF induction in rabbits

In order to investigate the role of the identified viral miRNAs in MCF, we chose to target the largest cluster of expressed miRNAs. Thus, we deleted all the cluster 2 miRNAs (miR-5 to miR-32) from the AlHV-1 BAC plasmid (Dewals *et al.*, 2006). Because the BAC cassette was initially inserted into the AlHV-miR-13 sequence, we could speculate that AlHV-miR-13 is not essential for MCF induction. However, expression of the entire cluster remained possible after excision of the BAC cassette, as observed in lymphoid tissue of MCF-developing rabbits infected with the AlHV-1 WT BAC-excised strain, with the exception of miR-13 (Fig. 3c, d). Cluster 2 miRNAs were therefore divided in two regions, from AlHV-1 miR-32 to miR-14 (left region) and from AlHV-1 miR-12 to miR-5 (right region) (Fig. 5a). We used an FLP/FRT-mediated approach in bacteria to first target the left region of the cluster before targeting the right region of

the cluster, as described in Methods. The molecular structures of the recombinant plasmids were confirmed by a combined *Eco*RI restriction endonuclease and Southern blotting approach (Fig. 5b). In the parental WT, the cluster 2 left and right regions were contained in two DNA fragments of approximately 13.8 and 14.6 kb, respectively. Replacement of the eGFPNeoR coding sequence by an ampicillin resistance gene sequence in the BAC cassette removed an *Eco*RI restriction site, resulting in two DNA fragments of 20.2 and 14.6 kb containing the cluster 2 miRNAs. This strategy was followed to impair off-target recombination into the neo/kanamycin resistance gene present in the BAC cassette. Deletion of the left and right regions of cluster 2 resulted in the disappearance of these two major hypermolar bands (Fig. 5b). The BAC WT eGFPNeoR[–]AmpR⁺ (WT) and miR^{FRT} plasmids were then used to reconstitute virions in MacT-Cre cells, resulting in Cre-mediated excision of the BAC cassette and viral propagation. Sequencing of the deleted regions confirmed the correct sequence in the targeted region in the recombinant miR^{FRT} virus (data not shown). To further verify that the deletion of cluster 2 miRNAs did not impact on ORF11 and/or ORF17 expression, we performed RT-PCR analyses targeting these two genes and confirmed their expression in infected BT cells (data not shown). Multiple-step growth-curve analyses revealed that the absence of cluster 2 miRNAs did not significantly affect viral growth *in vitro* (Fig. 5c).

To determine whether cluster 2 miRNAs are involved in the pathogenesis of MCF, rabbits were infected with WT or miR^{FRT} virus strains. Rabbits infected with the miR^{FRT} virus developed hyperthermia, hypertrophy of popliteal

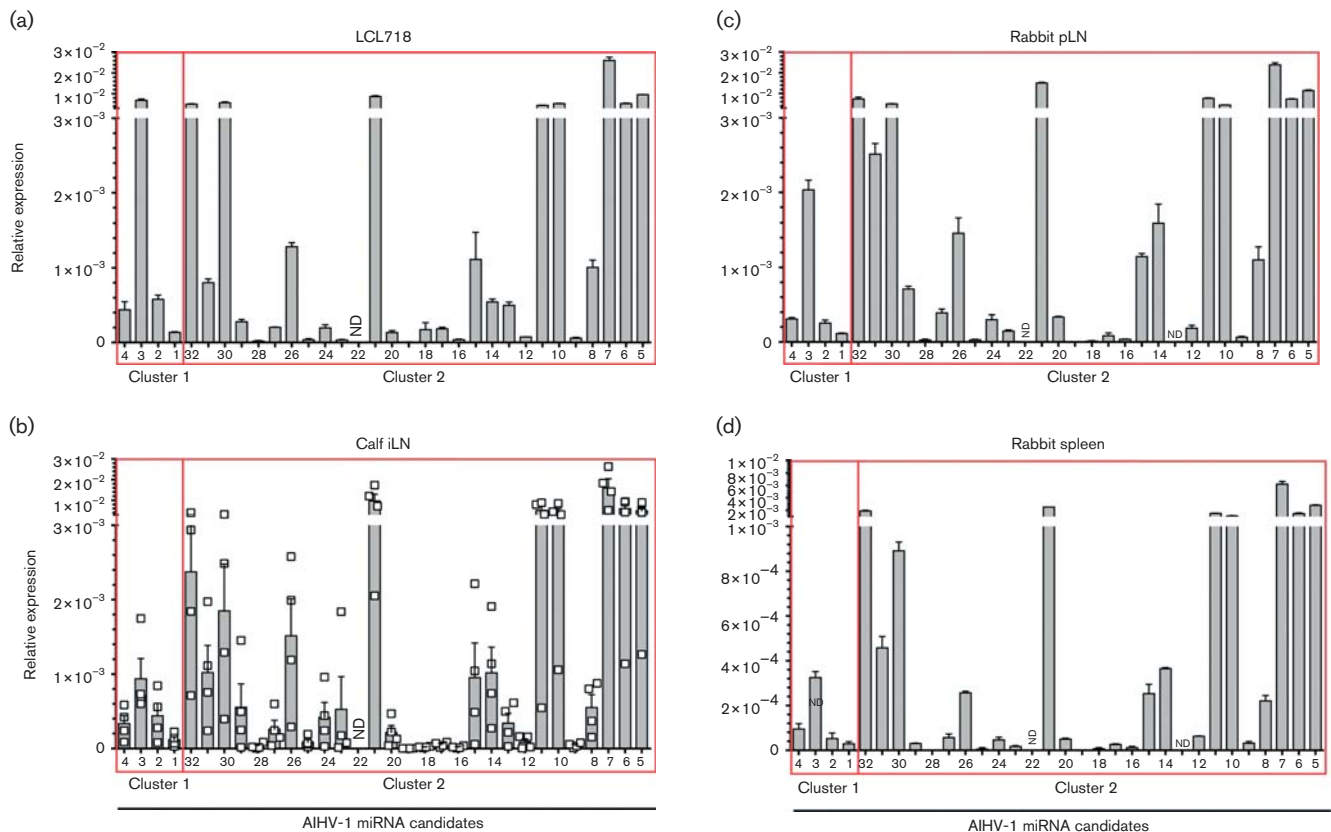


Fig. 3. Detection of AIHV-1 miRNA candidates by qRT-PCR. Total RNA (500 ng) was obtained from: (a) LCL718, (b) inguinal LN (iLN) of MCF-developing calves infected with the AIHV-1 WT C500 parental strain ($n=4$), open square symbols represent measurement for individual calves, (c) pLN cells of an MCF-developing rabbit infected with the AIHV-1 WT C500 BAC-excised strain, and (d) splenocytes of an MCF-developing rabbit infected with the AIHV-1 WT C500 BAC-excised strain. RNA was subjected to cDNA synthesis and miRNA-specific real-time PCR using a previously established protocol described in Methods (Balcells *et al.*, 2011). Mock-infected calves ($n=4$) were used as controls for PCR specificity. Expression of viral miRNAs relative to host miR-21 are shown as $2^{-\Delta Ct}$ values. Error bars indicate SE.

lymph nodes (pLNs) and spleen, and typical histopathological lesions, and did not survive the infection (Fig. 6a–d). The absence of cluster 2 miRNAs did not affect the induction of CD8⁺T cell expansion (Fig. 6e) and we observed similar viral loads at time of euthanasia in pLNs from rabbits infected with each virus strain by quantitative PCR and infectious centre assay (Fig. 6f, g). In addition, LCLs could be similarly propagated in the presence of IL-2 from LN cells isolated from WT or miR^{FRT}-infected rabbit pLNs. The obtained LCLs were mostly CD8⁺T cells (>90 %, data not shown). To further validate our approach, we performed qRT-PCR on total RNA extracted from the pLNs and spleen of MCF-developing rabbits infected with the miR^{FRT} virus. As expected, we observed expression of cluster 1 miRNAs but no detectable cluster 2 miRNAs (Fig. S4).

Taken together, these results demonstrated that at least 32 miRNAs are expressed during MCF in lymphoid tissues, but that the expression of 28 AIHV-1 miRNAs clustered in

a non-protein-coding region of the genome between ORF11 and ORF17 is not essential for virus replication or induction of MCF in rabbits. Although expression of these miRNAs was dispensable for MCF induction, further detailed analyses might reveal the effects of miRNAs that are not directly involved in the outcome of the disease. In addition, viral miRNAs are very poorly conserved. Consequently, even if rabbits develop clinical signs and lesions that are very similar to those observed in cattle, it remains possible that AIHV-1

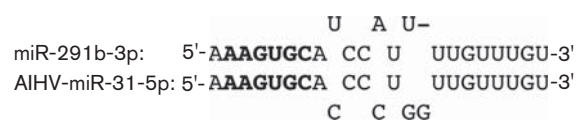


Fig. 4. Sequence comparison of AIHV-1 miR-31-5p and miR-291b-3p. Seed sequences are shown in bold.

miRNAs function differently in the context of bovine infection. Although it remains to be determined in future studies whether AIHV-1 miR-1 to 4 are involved in MCF, these results suggest that miRNAs that have been acquired by AIHV-1 during its coevolution with wildebeest could provide the fine regulation of viral and cellular gene expression occurring in latently infected cells to permit lifelong

persistence in the host species rather than being involved in a pathogenic mechanism leading to MCF.

METHODS

Cell lines and virus. Bovine turbinates (BT, ATCC CRL-1390) were cultured in Dulbecco's modified-essential medium (DMEM, Life

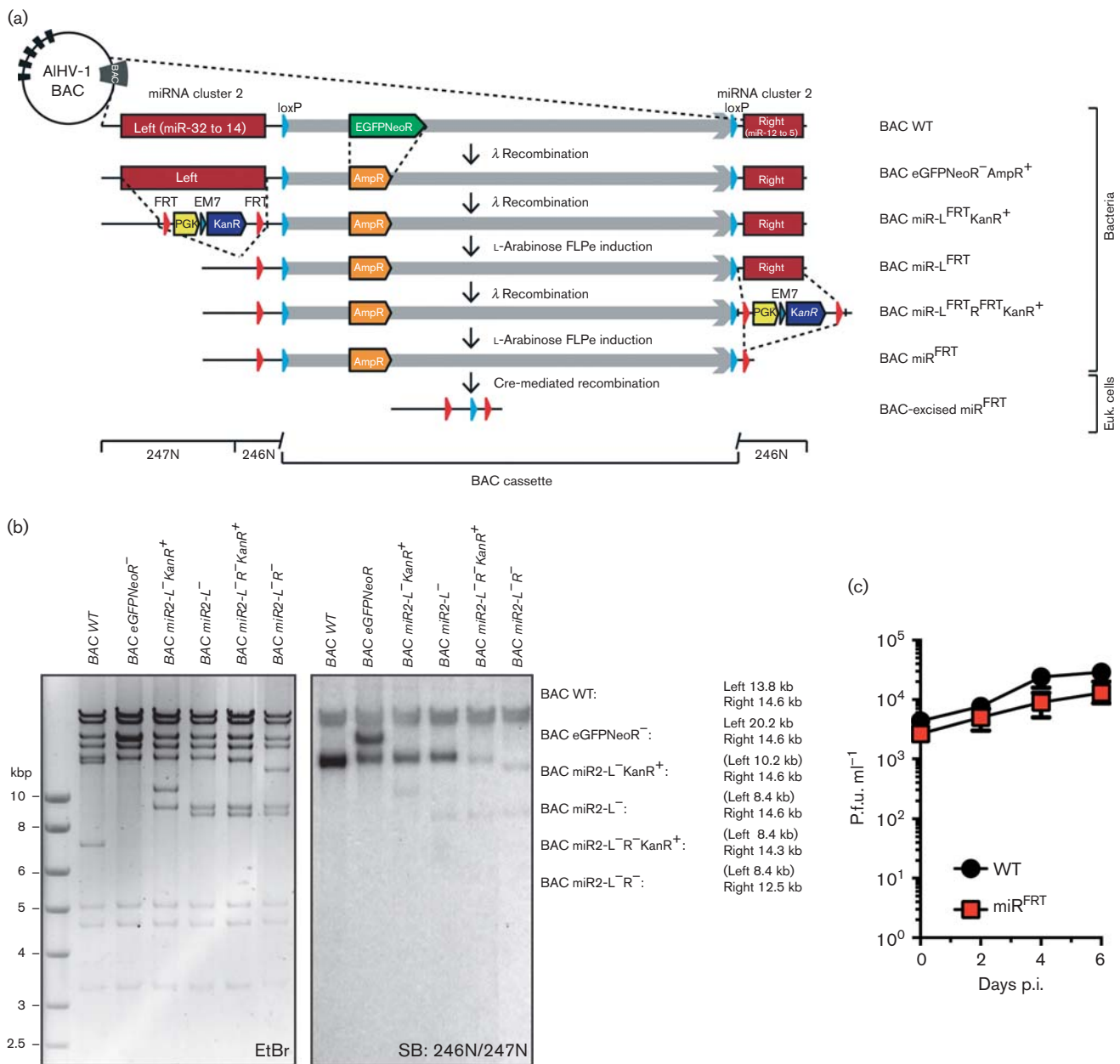


Fig. 5. Deletion of cluster 2 miRNAs. (a) Recombineering methodology used to delete cluster 2 miRNAs flanking the BAC cassette and generation of the miR^{FRT} strain. (b) Southern blotting analysis of produced BAC plasmid DNA after *Eco*RI restriction and ethidium bromide staining (EtBr). The probes corresponding to regions 246N and 247N were used (Ensner *et al.*, 1997). (c) Multi-step growth curves of WT and miR^{FRT} strains in BT fibroblasts. The data presented are means \pm SD of results from measurements in triplicate.

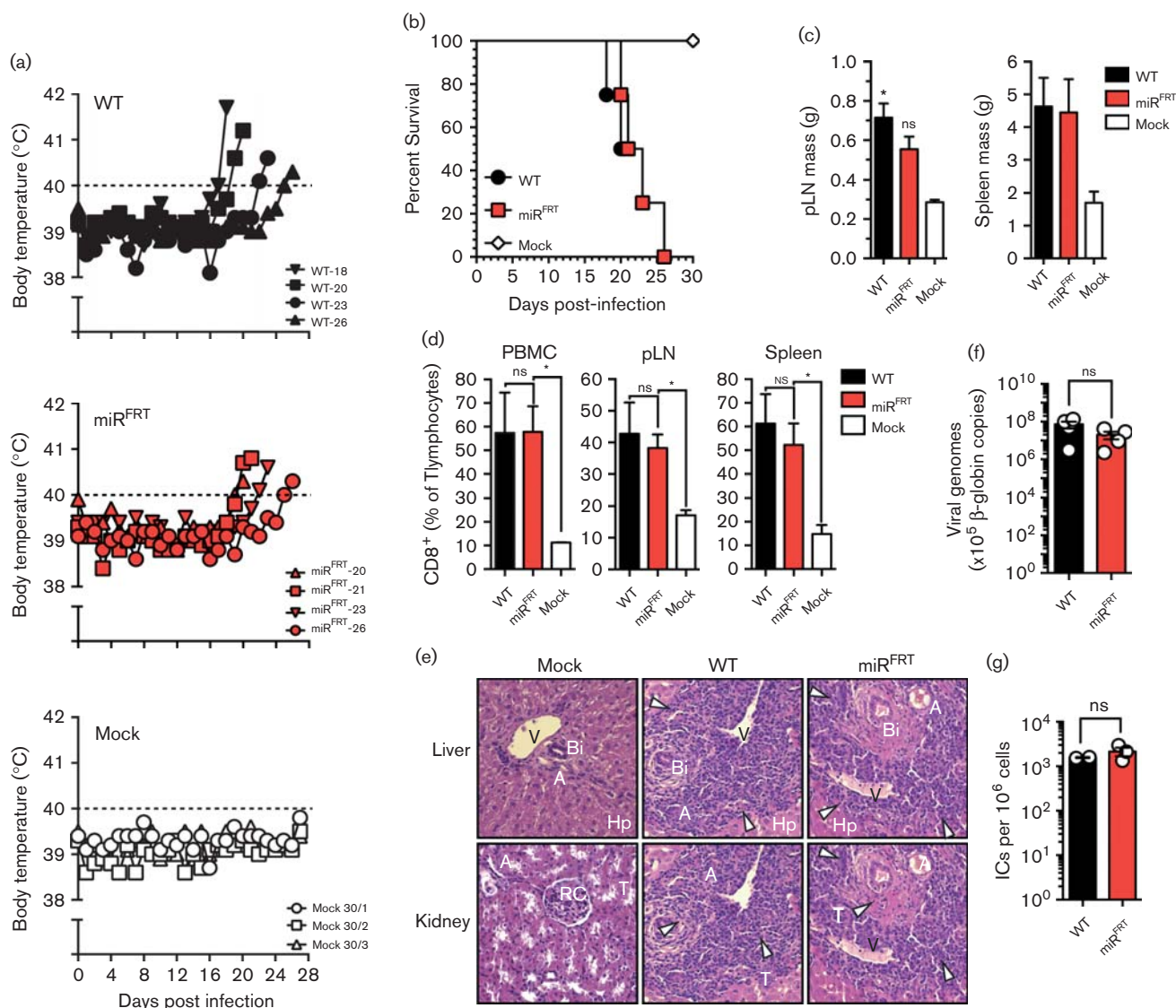


Fig. 6. AIHV-1 cluster 2 miRNAs are not involved in MCF pathogenesis. (a) Body temperature of three groups of rabbits infected intravenously with mock-infected BT cells (mock, $n=3$), or BT cells infected with the WT eGFPNeoR AmpR⁺ (WT, $n=4$) or miR^{FRT} ($n=4$) virus strains. (b) Cumulative incidence of survival. (c) Spleen and pLN mass at time of euthanasia. Bars represent mean \pm SE. * $P < 0.05$, ** $P < 0.01$, *** $P < 0.001$ (one-way ANOVA with Bonferroni's post test). (d) CD8⁺ cells (as a percentage of T lymphocytes) in the gated T cell population of PBMCs, pLNs and spleen analysed by flow cytometry at time of euthanasia. (e) Histopathological characterization of MCF lesions observed in liver and kidney of one rabbit representative of each group. White arrowheads indicate typical infiltrations of lymphoblastoid cells. A, arterioles; Bi, small bile ducts; Hp, hepatocytes; RC, renal corpuscles; T, uriniferous tubules; V, veins. (f) qPCR of viral genome copies in pLNs at time of euthanasia of rabbits infected with the recombinant strains. Real-time PCR quantification was normalized on 10^5 copies of β -globin cellular genomic sequence. Data are plotted as means \pm SE of triplicate measurements for each sample ($n=4$). Unpaired Student t -test. (g) Infectious centre (IC) assay per million cells of pLN. Data are plotted as means \pm SE of triplicate measurements for each sample ($n=4$). Unpaired Student t -test. NS, Not significant.

Technologies), supplemented with 10 % FCS (BioWhittaker). The pathogenic AIHV-1 C500 strain isolated from an ox with MCF and the AIHV-1 WT BAC clone were used in this study (Plowright *et al.*, 1975). Viruses were maintained by a limited number of passages (<5).

Animals. Calves were selected from a bovine herpesvirus 1, 4 and bovine viral diarrhoea virus (BVDV)-free herd in the Czech Republic.

All calves were screened 1 week after transportation at the Veterinary and Agrochemical Research Institute (Brussels, Belgium) and confirmed to be negative for the three viral pathogens mentioned above. The animals were allowed to acclimatize for 6 weeks and maintained on a diet of hay supplemented with minerals and concentrates.

Induction of MCF. Animals (calves or rabbits) were inoculated intravenously with $\sim 3 \times 10^6$ mock- or AIHV-1-infected BT cells, as

described previously (Palmeira *et al.*, 2013). According to bioethical rules, animals were euthanized 48 h after persistent hyperthermia ($>40^{\circ}\text{C}$). The local ethics committees of the CODA-CERVA and the University of Liège, for experiments involving calves or rabbits, respectively, have accredited the animal studies performed.

Propagation of AIHV-1-infected lymphoblastoid cell lines (LCL). Peripheral blood mononuclear cells (PBMCs) were isolated using Ficoll-Paque Premium density-gradient medium (GE Healthcare) as described earlier (Dewals *et al.*, 2011). Single-cell suspension (10^6 cells ml^{-1}) were then cultured in Iscove's modified Dulbecco's Medium (Life Technologies) containing 10 % FCS and 10 IU ml^{-1} recombinant human IL-2 (Roche). Medium was renewed every 3 days and cells were analysed by flow cytometry using a published procedure (Palmeira *et al.*, 2013) and used for RNA extraction and small RNA deep sequencing.

Small RNA cloning and sequencing. RNAs were extracted from AIHV-1-infected LCLs and from LN tissue of mock- or AIHV-1-infected calves developing MCF clinical signs by using TRI reagent (Ambion) as per the manufacturer's instructions. Small RNA cloning was conducted with 30 μg total RNA as previously described (Pfeffer *et al.*, 2005), except that PCR products were not concatenated and instead were sent directly for large-scale sequencing. Small RNA sequencing was performed at the Institut de Génétique et de Biologie Moléculaire et Cellulaire (IGBMC), Illkirch, France, using an Illumina Genome Analyser IIx instrument with a read length of 36 bp.

Processing and annotation of small RNA sequences. From an initial dataset of 35 404 509 reads, the data were clipped with the 3' adaptor TGGAATTCTCGGGTGCCAAGG, and trimmed. The reads were then collapsed into sequence tags and selected by size (>15 and <35 nt), which yielded a total of 2 425 556 unique sequence tags (collapsed reads). The sequence tags were then mapped to the genomes from which they may have been derived and to other already annotated RNAs by using Burrows–Wheeler Aligner (<http://bio-bwa.sourceforge.net>), permitting up to two mismatches per tag. The *Bos taurus* and AIHV-1 genome sequences were downloaded from the Ensembl repository (assembly version UMD3.1.67) and the RefSeq or GenBank database (accession numbers NC 002531 and AF005363 for the C500 strain long unique region and poly-repetitive terminal region, respectively), respectively. The following sources of annotated transcripts were used: miRBase v16 for miRNAs; Silva database for *B. taurus* rRNA; Genomic tRNA database for *B. taurus* tRNA; Noncode v2.0 database for *B. taurus* small nuclear-small nucleolar RNA (sn-snoRNA) and telomerase RNA; GenBank database for *B. taurus* small cytoplasmic RNA (scRNA) and Piwi-interacting RNA (piRNA); and Repbase v17.03 for *B. taurus* and common ancestral repeats. Thus, small RNAs that mapped unambiguously to sequences from one single functional category were easily classified, while the others were identified by applying the following annotation rule based on the abundances of various types of sequences in the cell: rRNA > tRNA > sn-snoRNA > miRNA > piRNA > repeat > pathogen genome > host genome > unknown.

Northern blotting. Total RNA was extracted from LCLs or LN tissue using TRI reagent (Ambion). Total RNA (10 μg) was mixed with an equal volume of RNA loading dye (1 \times TBE, pH 8.0, 12 % Ficoll, 0.01 % bromophenol blue, 0.02 % xylene cyanol FF, 7 M urea) and heated at 95°C for 5 min prior to separation in a pre-cast 15 % urea-acrylamide gel (Bio-Rad). RNA was transferred to a Hybond-NX membrane (GE Healthcare Lifesciences) in MilliQ water using a Transblot TURBO system (Bio-Rad) and chemically cross-linked at 60°C by using EDC [1-ethyl-3-(3-dimethylaminopropyl)carbodiimide hydrochloride] (Pierce) for 90 min, followed by extensive washing in

MilliQ water prior to prehybridization. Membranes were prehybridized for 2 h in PerfectHyb Plus solution (Sigma) at 42°C . For each candidate miRNA, antisense DNA oligonucleotides were 5'-end labelled with 25 μCi [γ - ^{32}P]dATP (Perkin Elmer) by using T4 polynucleotide kinase (NEB). The labelled probes were hybridized to the blot overnight at 42°C . The blot was then washed at 55°C twice for 10 min with low-stringency buffer ($5 \times \text{SSC}$ –0.1 % SDS), followed by a single wash in a higher-stringency buffer ($1 \times \text{SSC}$ –0.1 % SDS) for 5 min. Blotted membranes were then used to expose an Amersham Hyperfilm MP (GE Healthcare).

RT-PCR and quantitative PCR (qPCR). Reverse transcription (RT) reactions were performed in duplicate using total RNA as previously described (Balcells *et al.*, 2011). Briefly, 500 ng total RNA in a final volume of 10 μl including 1 μl of $10 \times$ poly(A) polymerase buffer containing 0.1 mM ATP, 1 mM each dNTP, 1 μM RT-primer (5'-CAGGTCCAGTTTTTTTTTTTTTTVN-3'), 80 U M-MLV reverse transcriptase (Bioo Scientific) and 0.75 U poly(A) polymerase (New England Biolabs) was incubated at 42°C for 1 h and 90°C for 5 min for enzyme inactivation. The cDNA obtained was then diluted to a final volume of 90 μl before further use. qPCR reactions were then performed on 3 μl diluted cDNA in a final volume of 20 μl including 10 μl iQ SYBR Green Supermix (Bio-Rad) and 200 nM each designed primer (Table S1). Reactions were performed using the protocol 95°C for 1 min, followed by 40 cycles of 95°C for 1 min and 58°C for 30 s, followed by melt-curve analysis (55 – 90°C in 0.5°C increments, with 3 s dwell time at each temperature) on a CFX96 Touch Real-Time PCR Detection System with CFX Manager v3 software (Bio-Rad). DNA primers for each selected miRNA candidate were designed using miRprimerdesign3 software (<http://tinyurl.com/qeo9a5o>) (Busk, 2014) (Table S1).

Mutagenesis. The AIHV-1 BAC clone was used to produce the recombinant plasmids using the pL451 plasmid vector containing an FRT-flanked expression cassette of the kanamycin/neomycin resistance gene as selection marker in *Escherichia coli* (Liu *et al.*, 2003) (<http://ncifrederick.cancer.gov/research/brb/recombineeringinformation.aspx>). To reduce off-target recombination events, the eGFPNeoR coding sequence in the BAC cassette (Dewals *et al.*, 2006) was replaced with a β -lactamase resistance gene amplified from the pGEMT Easy plasmid using chimeric primer pairs (Table S2, Fig. 5). The resulting WT eGFPNeoR⁺ BAC plasmid DNA was transformed in SW105 *E. coli* cells, encoding an L-arabinose-inducible FLPe recombinase (Warming *et al.*, 2005). The left region of the miRNA cluster 2 was then deleted by insertion of an amplicon consisting of a kanamycin-resistance gene cassette flanked by FRT sites and 50 bp homologous sequences, generated by PCR using the pL451 plasmid (Liu *et al.*, 2003) as template, and primers miR1L-PL451F and miR24L-PL451R (Table S2 and Fig. 5). The inserted kanamycin resistance cassette was excised following L-arabinose induction of the FLPe recombinase. Next, the right region of the miRNA cluster 2 was deleted by insertion of an amplicon consisting of a kanamycin resistance gene cassette flanked by FRT sites and 50 bp homologous sequences, generated by PCR using the pL451 plasmid as template, and primers miR24R-PL451F and miR32R-PL451R (Table S2, Fig. 5). The inserted kanamycin resistance cassette was subsequently excised following L-arabinose induction of the FLPe recombinase. All deletions and insertions were screened by PCR and verified by restriction profiles, Southern blot and sequencing of the recombination sites. The virus strains generated were reconstituted in MacT-cre cells before propagation in BT cells.

Growth curves. *In vitro* growth kinetics of miR^{FRT} virus were compared with those of the WT according to a published protocol (Palmeira *et al.*, 2013).

ACKNOWLEDGEMENTS

O.S. is a Research Fellow of the 'Fonds pour la formation à la Recherche dans l'Industrie et dans l'Agriculture' (FRIA). B.D. is a Research Associate of the 'Fonds de la Recherche Scientifique – FNRS'. A.V. is a member of the BELVIR consortium (IAP, phase VII) with a grant from the Belgian Science Policy Office (BELSPO, Belgium). The authors are grateful to the technical staff of the CODA-CERVA for the *in vivo* experiments in calves, as well as to Justine Javaux, Emeline Deglaire and Cédric Delforge for technical assistance (FARAH ULg). The authors thank Dr Benoît Muylkens (University of Namur) for helpful discussions. We thank the IGBMC Microarray and Sequencing platform, member of the France Genomique programme, for the sequencing of our libraries. This work was supported by the following grants: FSR-‘crédit classique’ from the University of Liège (C-13/97) and an Incentive Grant for Scientific Research ‘MAGIL’ from the F.R.S.-FNRS (F.4501.15).

REFERENCES

- Balcells, I., Cirera, S. & Busk, P. K. (2011). Specific and sensitive quantitative RT-PCR of miRNAs with DNA primers. *BMC Biotechnol* **11**, 70.
- Bartel, D. P. (2009). MicroRNAs: target recognition and regulatory functions. *Cell* **136**, 215–233.
- Barton, E., Mandal, P. & Speck, S. H. (2011). Pathogenesis and host control of gammaherpesviruses: lessons from the mouse. *Annu Rev Immunol* **29**, 351–397.
- Busk, P. K. (2014). A tool for design of primers for microRNA-specific quantitative RT-qPCR. *BMC Bioinformatics* **15**, 29.
- Buxton, D. & Reid, H. W. (1980). Transmission of malignant catarrhal fever to rabbits. *Vet Rec* **106**, 243–245.
- Chen, Y., Liersch, R. & Detmar, M. (2012). The miR-290-295 cluster suppresses autophagic cell death of melanoma cells. *Sci Rep* **2**, 808.
- Croce, C. M. (2009). Causes and consequences of microRNA dysregulation in cancer. *Nat Rev Genet* **10**, 704–714.
- Dewals, B. G. & Vanderplasschen, A. (2011). Malignant catarrhal fever induced by *Alcelaphine herpesvirus 1* is characterized by an expansion of activated CD3⁺CD8⁺CD4⁺T cells expressing a cytotoxic phenotype in both lymphoid and non-lymphoid tissues. *Vet Res* **42**, 95.
- Dewals, B., Boudry, C., Gillet, L., Markine-Goriaynoff, N., de Leval, L., Haig, D. M. & Vanderplasschen, A. (2006). Cloning of the genome of *Alcelaphine herpesvirus 1* as an infectious and pathogenic bacterial artificial chromosome. *J Gen Virol* **87**, 509–517.
- Dewals, B., Boudry, C., Farnir, F., Drion, P. V. & Vanderplasschen, A. (2008). Malignant catarrhal fever induced by alcelaphine herpesvirus 1 is associated with proliferation of CD8⁺T cells supporting a latent infection. *PLoS One* **3**, e1627.
- Dewals, B., Myster, F., Palmeira, L., Gillet, L., Ackermann, M. & Vanderplasschen, A. (2011). *Ex vivo* bioluminescence detection of *Alcelaphine herpesvirus 1* infection during malignant catarrhal fever. *J Virol* **85**, 6941–6954.
- Diebel, K. W., Oko, L. M., Medina, E. M., Niemeyer, B. F., Warren, C. J., Claypool, D. J., Tibbetts, S. A., Cool, C. D., Clambey, E. T. & van Dyk, L. F. (2015). Gammaherpesvirus small noncoding RNAs are bifunctional elements that regulate infection and contribute to virulence *in vivo*. *MBio* **6**, e01670–e01714.
- Dölken, L., Krmpotic, A., Kothe, S., Tuddenham, L., Tanguy, M., Marciniowski, L., Ruzsics, Z., Elefant, N., Altuvia, Y. & other authors (2010). Cytomegalovirus microRNAs facilitate persistent virus infection in salivary glands. *PLoS Pathog* **6**, e1001150.
- Ensser, A. & Fleckenstein, B. (2005). T-cell transformation and oncogenesis by γ 2-herpesviruses. *Adv Cancer Res* **93**, 91–128.
- Ensser, A., Pflanz, R. & Fleckenstein, B. (1997). Primary structure of the alcelaphine herpesvirus 1 genome. *J Virol* **71**, 6517–6525.
- Feederle, R., Linnstaedt, S. D., Bannert, H., Lips, H., Bencun, M., Cullen, B. R. & Delecluse, H. J. (2011). A viral microRNA cluster strongly potentiates the transforming properties of a human herpesvirus. *PLoS Pathog* **7**, e1001294.
- Feldman, E. R., Kara, M., Coleman, C. B., Grau, K. R., Oko, L. M., Krueger, B. J., Renne, R., van Dyk, L. F. & Tibbetts, S. A. (2014). Virus-encoded microRNAs facilitate gammaherpesvirus latency and pathogenesis *in vivo*. *MBio* **5**, e00981–e001014.
- Gottwein, E., Mukherjee, N., Sachse, C., Frenzel, C., Majoros, W. H., Chi, J. T., Braich, R., Manoharan, M., Soutschek, J. & other authors (2007). A viral microRNA functions as an orthologue of cellular miR-155. *Nature* **450**, 1096–1099.
- Grey, F. (2015). Role of microRNAs in herpesvirus latency and persistence. *J Gen Virol* **96**, 739–751.
- Kincaid, R. P. & Sullivan, C. S. (2012). Virus-encoded microRNAs: an overview and a look to the future. *PLoS Pathog* **8**, e1003018.
- Liu, P., Jenkins, N. A. & Copeland, N. G. (2003). A highly efficient recombineering-based method for generating conditional knockout mutations. *Genome Res* **13**, 476–484.
- Lüningschrör, P., Stöcker, B., Kaltschmidt, B. & Kaltschmidt, C. (2012). miR-290 cluster modulates pluripotency by repressing canonical NF- κ B signaling. *Stem Cells* **30**, 655–664.
- Nightingale, K., Levy, C. S., Hopkins, J., Grey, F., Esper, S. & Dalziel, R. G. (2014). Expression of ovine herpesvirus-2 encoded microRNAs in an immortalised bovine - cell line. *PLoS One* **9**, e97765.
- Palmeira, L., Sorel, O., Van Campe, W., Boudry, C., Roels, S., Myster, F., Reschner, A., Coulie, P. G., Kerkhofs, P. & other authors (2013). An essential role for γ -herpesvirus latency-associated nuclear antigen homolog in an acute lymphoproliferative disease of cattle. *Proc Natl Acad Sci U S A* **110**, E1933–E1942.
- Pfeffer, S., Zavolan, M., Grässer, F. A., Chien, M., Russo, J. J., Ju, J., John, B., Enright, A. J., Marks, D. & other authors (2004). Identification of virus-encoded microRNAs. *Science* **304**, 734–736.
- Pfeffer, S., Sewer, A., Lagos-Quintana, M., Sheridan, R., Sander, C., Grässer, F. A., van Dyk, L. F., Ho, C. K., Shuman, S. & other authors (2005). Identification of microRNAs of the herpesvirus family. *Nat Methods* **2**, 269–276.
- Plowright, W. I. (1965a). Malignant catarrhal fever in East Africa. I. Behaviour of the virus in free-living populations of blue wildebeest (*Gorgon taurinus taurinus* Burchell). *Res Vet Sci* **6**, 56–68.
- Plowright, W. (1965b). Malignant catarrhal fever in East Africa. II. Observations on wildebeest calves at the laboratory and contact transmission of the infection to cattle. *Res Vet Sci* **6**, 69–83.
- Plowright, W. (1990). Malignant catarrhal fever virus. In *Virus Infections of Ruminants*, pp. 123–150. Edited by Z. Dinter & B. Morein. Amsterdam: Elsevier.
- Plowright, W., Ferris, R. D. & Scott, G. R. (1960). Blue wildebeest and the aetiological agent of bovine malignant catarrhal fever. *Nature* **188**, 1167–1169.
- Plowright, W., Herniman, K. A., Jessett, D. M., Kalunda, M. & Rampton, C. S. (1975). Immunisation of cattle against the herpesvirus of malignant catarrhal fever: failure of inactivated culture vaccines with adjuvant. *Res Vet Sci* **19**, 159–166.
- Riaz, A., Dry, I., Levy, C. S., Hopkins, J., Grey, F., Shaw, D. J. & Dalziel, R. G. (2014). Ovine herpesvirus-2-encoded microRNAs target virus genes involved in virus latency. *J Gen Virol* **95**, 472–480.

- Rosewick, N., Momont, M., Durkin, K., Takeda, H., Caiment, F., Cleuter, Y., Vernin, C., Mortreux, F., Wattel, E. & other authors (2013). Deep sequencing reveals abundant noncanonical retroviral microRNAs in B-cell leukemia/lymphoma. *Proc Natl Acad Sci U S A* **110**, 2306–2311.
- Russell, G. C., Stewart, J. P. & Haig, D. M. (2009). Malignant catarrhal fever: a review. *Vet J* **179**, 324–335.
- Seto, E., Moosmann, A., Grömminger, S., Walz, N., Grundhoff, A. & Hammerschmidt, W. (2010). Micro RNAs of Epstein-Barr virus promote cell cycle progression and prevent apoptosis of primary human B cells. *PLoS Pathog* **6**, e1001063.
- Stik, G., Laurent, S., Coupeau, D., Coutaud, B., Dambrine, G., Rasschaert, D. & Muykens, B. (2010). A p53-dependent promoter associated with polymorphic tandem repeats controls the expression of a viral transcript encoding clustered microRNAs. *RNA* **16**, 2263–2276.
- Suffert, G., Malterer, G., Hausser, J., Viiläinen, J., Fender, A., Contrant, M., Ivacevic, T., Benes, V., Gros, F. & other authors (2011). Kaposi's sarcoma herpesvirus microRNAs target caspase 3 and regulate apoptosis. *PLoS Pathog* **7**, e1002405.
- Swa, S., Wright, H., Thomson, J., Reid, H. & Haig, D. (2001). Constitutive activation of Lck and Fyn tyrosine kinases in large granular lymphocytes infected with the γ -herpesvirus agents of malignant catarrhal fever. *Immunology* **102**, 44–52.
- Tuddenham, L., Jung, J. S., Chane-Woon-Ming, B., Dölken, L. & Pfeffer, S. (2012). Small RNA deep sequencing identifies microRNAs and other small noncoding RNAs from human herpesvirus 6B. *J Virol* **86**, 1638–1649.
- Ventura, A. & Jacks, T. (2009). MicroRNAs and cancer: short RNAs go a long way. *Cell* **136**, 586–591.
- Walz, A., Feinstein, P., Khan, M. & Mombaerts, P. (2007). Axonal wiring of guanylate cyclase-D-expressing olfactory neurons is dependent on neuropilin 2 and semaphorin 3F. *Development* **134**, 4063–4072.
- Walz, N., Christalla, T., Tessmer, U. & Grundhoff, A. (2010). A global analysis of evolutionary conservation among known and predicted gammaherpesvirus microRNAs. *J Virol* **84**, 716–728.
- Warming, S., Costantino, N., Court, D. L., Jenkins, N. A. & Copeland, N. G. (2005). Simple and highly efficient BAC recombineering using *galK* selection. *Nucleic Acids Res* **33**, e36.
- Zhao, Y., Yao, Y., Xu, H., Lambeth, L., Smith, L. P., Kgosana, L., Wang, X. & Nair, V. (2009). A functional microRNA-155 ortholog encoded by the oncogenic Marek's disease virus. *J Virol* **83**, 489–492.
- Zhao, Y., Xu, H., Yao, Y., Smith, L. P., Kgosana, L., Green, J., Petherbridge, L., Baigent, S. J. & Nair, V. (2011). Critical role of the virus-encoded microRNA-155 ortholog in the induction of Marek's disease lymphomas. *PLoS Pathog* **7**, e1001305.
- Zhu, Y., Haecker, I., Yang, Y., Gao, S. J. & Renne, R. (2013). γ -Herpesvirus-encoded miRNAs and their roles in viral biology and pathogenesis. *Curr Opin Virol* **3**, 266–275.
- Zuker, M. (2003). Mfold web server for nucleic acid folding and hybridization prediction. *Nucleic Acids Res* **31**, 3406–3415.